



Flame retardant and thermal degradation properties of flame retardant thermoplastic polyurethane based on HGM@[EOOEMIm][BF₄]

Chuanmei Jiao¹ · Hongzhi Wang¹ · Xilei Chen¹ · Guowu Tang²

Received: 26 March 2018 / Accepted: 24 June 2018 / Published online: 13 July 2018
© Akadémiai Kiadó, Budapest, Hungary 2018

Abstract

This article mainly studies the flame retardant and thermal degradation properties of thermoplastic polyurethane (TPU) composites based on HGM@[EOOEMIm][BF₄], prepared by modifying hollow glass microsphere (HGM) with ionic liquid [EOOEMIm][BF₄]. The physical and chemical characteristic of HGM@[EOOEMIm][BF₄] was tested by X-ray photoelectron spectroscopy and scanning electron microscope–energy-dispersive spectrometer, respectively. And then the flame retardant and thermal degradation characteristics of all TPU composites were tested using smoke density test (SDT), cone calorimeter test (CCT) and thermogravimetric/fourier transform infrared spectroscopy, etc. The SDT results showed that HGM@[EOOEMIm][BF₄] can significantly decrease the amount of smoke production. The CCT revealed that HGM@[EOOEMIm][BF₄] can greatly enhance the flame retardant of TPU. The peak heat release rate value decreased from 1224.0 kW m⁻² (TPU0) to 498.5 kW m⁻² (TPU/HB2). The TG test showed that HGM@[EOOEMIm][BF₄] can improve the thermal stability of TPU composites and promote the char formation in the combustion process of TPU. All results confirmed that HGM@[EOOEMIm][BF₄] can make a great influence on the combustion and degradation of TPU.

Keywords Thermal degradation · Thermoplastic polyurethane · Hollow glass microspheres · [EOOEMIm][BF₄]

Introduction

Thermoplastic polyurethane (TPU) is a versatile engineering thermoplastics with high tension, flexural fatigue strength, excellent low temperature flexibility and abrasion resistance, which has been widely used in many fields such as coatings, footwear, furniture and insulation materials [1]. However, the same as many other thermoplastics, the flame retardant properties are reduced due to its inherent flammability that burns in a rapid way and generates a large amount of smoke during combustion, which has also

limited the application of TPU. Therefore, it is of great importance to improve the flame retardancy of TPU [2].

Many measures have been made to improve the flame retardancy of TPU at present [3–5]. And, it has been illustrated that the most simple and effective ways to improve the flame retardant performance of TPU is to add flame retardants into it, and have achieved a good effect. For example, halogen flame retardants were widely applied in TPU to improve the fire safety. However, it has been limited in some special fields due to its fatal disadvantages releasing a lot of smoke, toxic and corrosive gases during combustion [6]. Thus, the halogen-free flame retardants with low smoke and low toxicity have become the trend, and have achieved a good improvement in fire safety.

Hollow glass microsphere (HGM) is a special type of inorganic and spherical powder material with large surface area, low density, low dielectric constant and thermal conductivity, which consists of outer stiff glass and inner inert gas [7]. The hollow structure endows HGM excellent thermal insulating property. Based on these properties, HGM has significant application prospects in aerospace

✉ Chuanmei Jiao
jiaochm@qust.edu.cn

¹ College of Environment and Safety Engineering, Qingdao University of Science and Technology, Qingdao 266042, Shandong, People's Republic of China

² College of Chemistry, Chemical Engineering and Materials Science, Institute of Molecular and Science, Shandong Normal University, Jinan 250014, Shandong, People's Republic of China

[8], deep-sea exploration [9] and hydrogen storage [10, 11] and so on. In previous research, HGM, as fillers, was mainly used in the fabrication of polymer composite materials for different applications in the insulation area [12–14]. But up to date, given the amount of research work published on the properties of HGM application; little work has been found for the work about HGM applied in the flame retardant fields. In our previous work, HGM was used as a synergistic agent with aluminum hydroxide or magnesium hydroxide in flame retardant EVA composites [7, 15], confirming that HGM can improve the flame retardancy of EVA composites by changing the structure of char residue. HGM has also been introduced into TPU alone, and it is found that HGM can make the structures of char residue compact and hard and significantly increase the flame retardant property of TPU [16]. Ionic liquids (ILs), with good properties just like low melting point, high heat stability and incombustibility, have been widely used in various fields of chemical research [16–18]. According to the reports, the ILs had catalytic effect on Friedel–Crafts reaction, further promoting char cross-linking formation of materials and increasing the flame retardancy of materials [19, 20]. [EOOEMIm][BF₄], as one of the important ILs with all the properties of ILs, contains F and B flame retardant elements, which may have good flame retardancy for TPU. Combining HGM with [EOOEMIm][BF₄], a new flame retardant maybe be obtained. To the best of our knowledge, there is no report about the combination between HGM and [EOOEMIm][BF₄] used as flame retardant for TPU.

In this paper, HGM@[EOOEMIm][BF₄], a new type of flame retardant, was prepared by modifying HGM with [EOOEMIm][BF₄], and applied in TPU by molten blending method. The structure of HGM@[EOOEMIm][BF₄] was confirmed using a series of tests including XPS, SEM and EDS. Then, the flame retardant and thermal degradation properties of the composites based on TPU and HGM@[EOOEMIm][BF₄] were intensively studied by SDT, CCT and TG–IR, respectively.

Experimental

Materials

TPU (9380A) was produced by Bayer Germany, and the basic properties of TPU are as follows: hardness: 82A (ISO868); density: 1.110 g cm⁻³ (ISO1183); tensile strength: 40 MPa (ISO527-1, -3); and elongation at break: 500% (ISO527-1, -3). HGM composed of sodium borosilicate (grade: 5020, production place: Australia, particle size: 15–150 μm, medium particle: 50 μm, density: 0.2 g cm⁻³) was obtained from Guangzhou Qingcong

trading Co, Ltd. 1-((ethoxycarbonyl)methyl)-3-methylimidazolium tetrafluoroborate ([EOOEMIm][BF₄]) was purchased from Lanzhou Institute of Chemical Physics, Chinese Academy of Sciences. Basic properties parameters are as follows: molecular formula: C₈H₁₃BF₄N₂O₂; molecular weight: 256.01; purity: ≥ 98%.

Synthesis of HGM@[EOOEMIm][BF₄]

First, 15 g HGM is activated in hydrochloric acid (HCl) for 10 min. Then, HGM was put in an ultrasonic cleaner to maintain washing for about half an hour, after that, washed and dried in vacuum drying oven, respectively. Then, the treated HGM, silane coupling agent KH550 (20%, 15 mL) and the mixed solvent of triethylamine ((C₂H₅)₃N, 1.5 mL, as catalyst) and acetonitrile (CH₃CN, 300 mL, as a reaction solvent) were poured into a three-neck flask equipped with a stirrer and reflux device under a nitrogen atmosphere. After that, the mixture was heated to 60 °C. During the reaction process, some HGM particles were easily dispersed in the liquid phase. Meanwhile, some particles well dispersed in acetonitrile. The reaction was stirring for 24 h. Then, the reaction mixture was cooled down to room temperature, filtered and washed with acetonitrile (30 mL), ethanol (500 mL), ultra-pure water (500 mL), and then the sample was dried in a vacuum oven at 80 °C for 8 h. The above modified HGM (5 g) was put into acetonitrile solvent (30 mL) in flask, and excess [EOOEMIm][BF₄] (3.0 g) was added into the flask, and mixed for 24–36 h. After that, HGM@[EOOEMIm][BF₄] was obtained after filtering, washing and drying process. The synthesis process is given in Scheme 1.

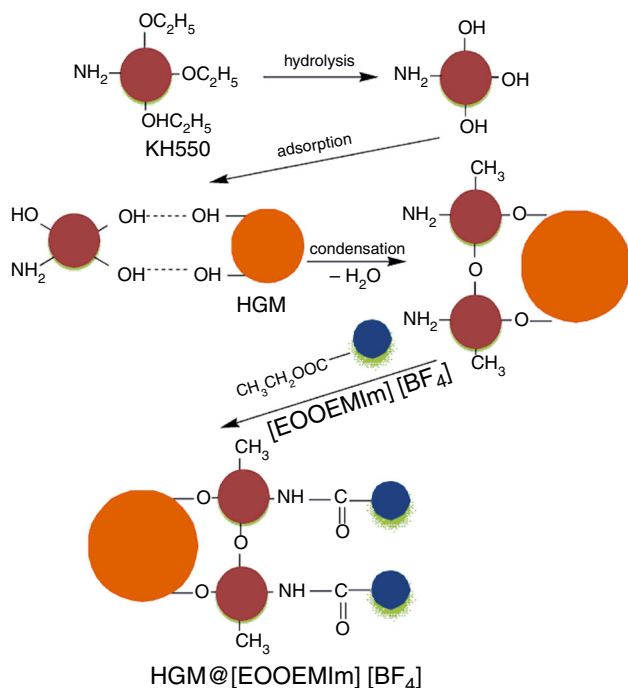
Sample preparation

TPU was dried in a vacuum oven at 80 °C for 24 h. Then, TPU mixed with HGM@[EOOEMIm][BF₄] in different ratios (the formulations are given in Table 1), the quality of each group was 80 g, added to the internal mixer (SU-70B) with the rotation speed of 30 rpm for 10 min. The materials from the internal mixer were put into the tablet machine (the quality of materials for each sample is 45 g with the size 10 × 10 × 3 mm³) with the temperature of the splints was both 180 °C.

Measurements

X-ray photoelectron spectroscopy (XPS)

The XPS spectra were recorded with a VG Escalab mark II spectrometer (VG Scientific Ltd, UK), using Al Kα excitation radiation ($h\nu = 1253.6$ eV) and calibrated by



Scheme 1 Synthesis process of HGM@[EOOEMIm][BF₄]

assuming the binding energy of carbonaceous carbon to be 284.6 eV.

Scanning electron microscope–energy-dispersive spectrometer (SEM–EDS)

The surface morphologies of HGM and HGM@[EOOEMIm][BF₄] were observed using a JEOL JSM 6700 LV scanning electron microscope (SEM) (JEOL, Japan) at an accelerating voltage of 5 and 8 kV.

Smoke density test (SDT)

The smoke density test (Qingdao University of Science and Technology; Naer Company in Dong Guan) was used to measure the smoke production properties according to ISO 5659-2. The samples with the dimension of 75 × 75 × 3 mm³ were exposed to a radiant cone at a heat flux of 25 kW m⁻², 552 °C.

Cone calorimeter test (CCT)

The flame retardant properties of the samples were measured by a cone calorimeter device (Fire Testing Technology, UK) according to ISO 5660 standard procedures. The samples with the dimension of 100 × 100 × 3 mm³ were exposed to a radiant cone at a heat flux of 35 kW m⁻². And the samples mass was 50 ± 2 g.

Thermogravimetric analysis/infrared spectrometry (TG–IR)

Thermogravimetric analysis/infrared spectrometry (TG–IR) of the pure TPU and flame retardant TPU was performed using a DT-50 (Setaram, France) instrument that was interfaced to an IRAffinity-1 FT-IR spectrometer. About 10.0 mg of sample was put in an alumina crucible and heated from 30 to 700 °C. The heating rate was set as 20 K min⁻¹ (nitrogen atmosphere, flow rate of 60 mL min⁻¹).

Results and discussion

Characterization of HGM@[EOOEMIm][BF₄]

XPS

XPS was used to characterize the surface chemical state of neat HGM and HGM@[EOOEMIm][BF₄] and determined the evidence of modification [21]. The results of XPS are shown in Fig. 1. The peak at 192.5 eV indicated B_{1s} on the surfaces of both HGM and HGM@[EOOEMIm][BF₄] due to the fact that the main component of HGM is borosilicate. However, the B_{1s} counts of HGM@[EOOEMIm]

[BF₄] increased after modified by [EOOEMIm][BF₄]. Compared with HGM, a new peak appeared at 688 eV for HGM@[EOOEMIm][BF₄], which was attributed to the binding energy of F_{1s}, proving that [EOOEMIm][BF₄] was grafted onto the surface of HGM. HGM@[EOOEMIm][BF₄] may show good flame retardant effects because of the incorporation of [EOOEMIm][BF₄] containing flame retardant elements, such as F, N and B.

Table 1 Formulations of flame retardant TPU composites

Sample code	TPU/mass%	HGM@[EOOEMIm][BF ₄]/mass%	HGM/mass%
TPU0	100.000	0.000	0.000
TPU/H1	99.875	0.000	0.125
TPU/H2	99.750	0.000	0.250
TPU/HB1	99.850	0.125	0.000
TPU/HB2	99.750	0.250	0.000

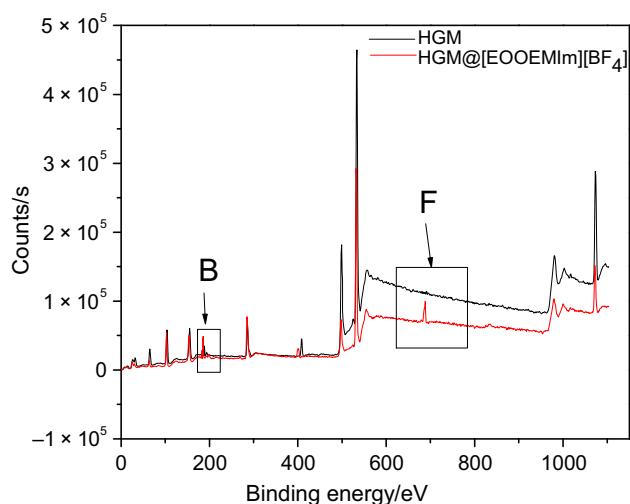


Fig. 1 XPS spectra of HGM and HGM@[EOOEMIm][BF₄]

SEM-EDS

The SEM-EDS was used to further confirm the structure of HGM@[EOOEMIm][BF₄], and the results are presented in Fig. 2a, b. It can be seen from Fig. 2, the surface of HGM particles was very smooth (as shown in picture A and B). However, a much rough surface of HGM@[EOOEMIm][BF₄] was obtained after the modification (as shown in picture A' and B'), indicating that [EOOEMIm][BF₄] has been successfully grafted onto the surface of HGM during the synthesis process. The EDS results of HGM and HGM@[EOOEMIm][BF₄] are given in Fig. 2b. Compared to the HGM, the B element content of HGM@[EOOEMIm][BF₄] was much higher than HGM. And, the amount of F on the surface of HGM@[EOOEMIm][BF₄] was considerable. The above results further confirmed the success of modification.

Smoke density test

Smoke performance of the composite is a very important parameter in flame retardant fields. The smoke density test (SDT) is often used to estimate the smoke suppression characteristics of the composites and give the detailed information about the smoke production [22]. The luminous flux (LF) parameter from SDT can be used to measure the amount of smoke production.

Figure 3 presented the LF curves of TPU composites in the SDT without (A)/with (B) flame. From Fig. 3a, it could be seen that the LF of TPU0 rapidly decreased after 265 s and attained the lowest value (2.7%) at 1200 s. In the case of TPU/H1 with only 0.125 mass% HGM, the LF greatly decreased after 240 s and reached the lowest LF value (4.2%) at the end of the experiment, which was apparently higher than that of TPU0. For TPU/HB1 with the same

loading of HGM@[EOOEMIm][BF₄], the LF attained the lowest value of 8.9%, which was increased by 111.9% compared with TPU/H1. When 0.25 mass% of HGM (TPU/H2) and 0.25 mass% of HGM@[EOOEMIm][BF₄] (TPU/HB2) were added into TPU, the lowest LF values were 10.9 and 15.6%, respectively. Obviously, the LF value of TPU/HB2 was higher than that of TPU/H2. It should be figured out that the time for the initial reduction in LF became short with the addition of HGM or HGM@[EOOEMIm][BF₄]. This can be interpreted that HGM and HGM@[EOOEMIm][BF₄] could catalyze TPU to decompose at low temperature to form smoke precursor and char residue shell. Furthermore, they could migrate onto the surface of the sample and change the structure of char residue. So, the production rate of smoke precursor would decrease due to the formation of char residue shell as barrier. However, it should be noted that the smoke suppression effect of HGM@[EOOEMIm][BF₄] is more apparent than HGM. That was due to the fact that [EOOEMIm][BF₄] had catalytic effect on Friedel-Crafts reaction, further promoting char formation and increasing the stability of the char layer during the process of pyrolysis and combustion [19].

Figure 3b shows the LF curves of TPU composites with flame. In the case of TPU0, the LF rapidly decreased after 225 s and got the lowest LF value (0.9%) at 760 s, but then slightly increased gradually and reached to 2.1% at the end of the experiment. The reason is that smoke particles begin to reunite and settle, which results the LF curve of TPU0 like saddle shape. The same as the condition without flame, the LF of the composites containing HGM@[EOOEMIm][BF₄] further increased compared with composites containing HGM. It can be concluded that there is an apparently smoke suppression for HGM@[EOOEMIm][BF₄] applied in TPU.

Cone calorimeter test

Heat release rate (HRR)

HRR is a very important parameter to express the intensity of a fire [23]. And the peak HRR (pHRR) is often used to describe the combustion behavior for actual situation. The HRR curves are shown in Fig. 4. It could be seen that a sharp HRR curve for TPU0 appeared at the range of 50–350 s, with a pHRR value of 1224.0 kW m⁻². When 0.125 and 0.25 mass% of HGM were added into TPU, the pHRR values were 747.2 and 597.0 kW m⁻², reduced by 39.0 and 51.2% compared with pure TPU, respectively. However, when the loading of HGM@[EOOEMIm][BF₄] was 0.125 mass% (TPU/HB1) and 0.25 mass% (TPU/HB2), the pHRR values were 642.1 and 498.5 kW m⁻², which were lower than those of TPU/H1 and TPU/H2 with

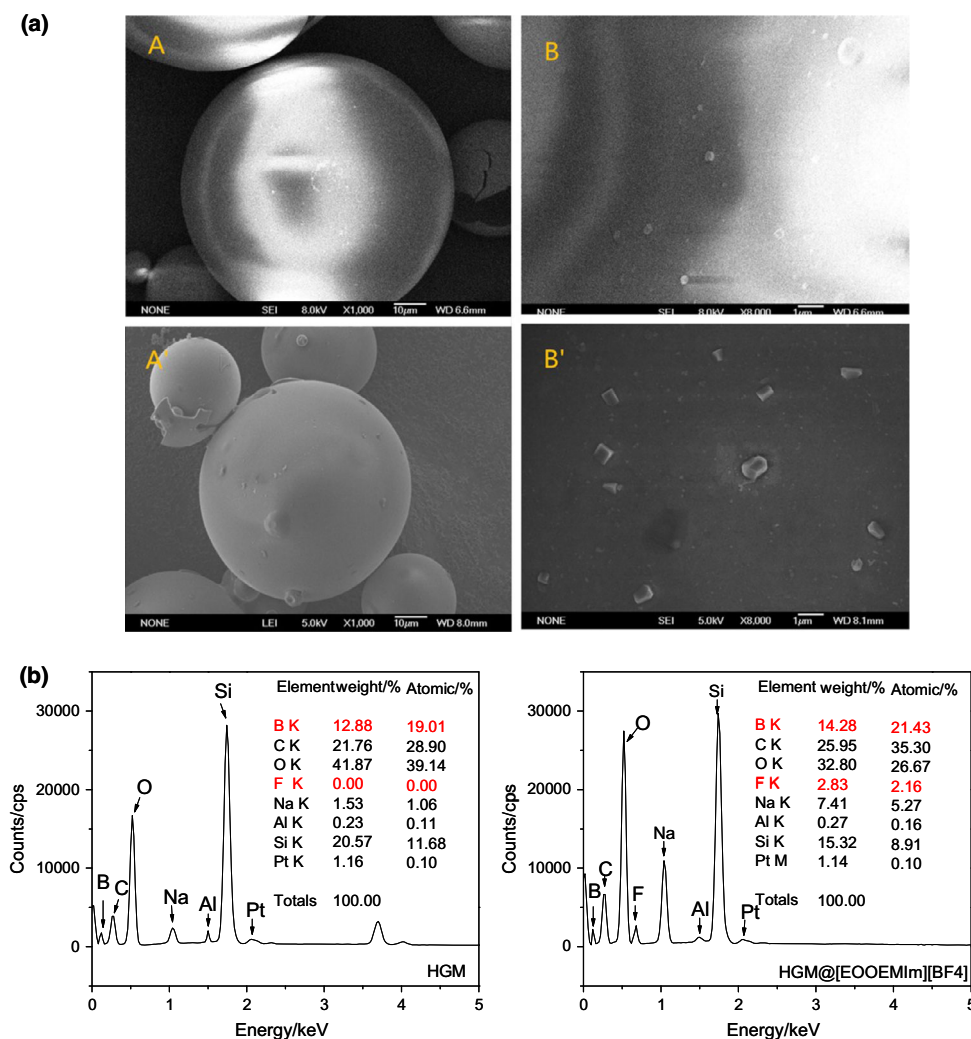


Fig. 2 **a** The SEM results of HGM and HGM@[EOOEMIm][BF₄]. **b** The EDS results of HGM and HGM@[EOOEMIm][BF₄]

the same content of HGM. This means HGM@[EOOEMIm][BF₄] has a better effect in reducing the heat release compared with HGM. The reason is that both HGM and HGM@[EOOEMIm][BF₄] can migrate progressively onto the surface of the TPU, and change char residue layer preventing heat and mass transfer between underlying materials and flame zone, thus reduced the HRR [24]. In the case of the samples containing HGM@[EOOEMIm][BF₄], [EOOEMIm][BF₄] on the surface of HGM can further promote the char formation and change the structure of char residue. In addition, there are B and F flame retardant elements in HGM@[EOOEMIm][BF₄], which can further improve the flame retardant effect.

Total heat release (THR)

The THR curves of TPU composites are shown in Fig. 5. It can be found that the THR value of TPU was 183.0 MJ m⁻², which is higher than those of TPU composites with HGM or HGM@[EOOEMIm][BF₄]. Comparing TPU/H1 with TPU/HB1 at the same loading content (0.125 mass%), the THR of TPU/HB1 (127.3 MJ m⁻²) was lower than that of TPU/H1 (157.4 MJ m⁻²). And for the samples with 0.25 mass% HGM and 0.25 mass% HGM@[EOOEMIm][BF₄], the THR decreased from 145.3 MJ m⁻² (TPU/H2) to 127.3 MJ m⁻². Obviously, the THR value of samples containing HGM@[EOOEMIm][BF₄] was lower than samples

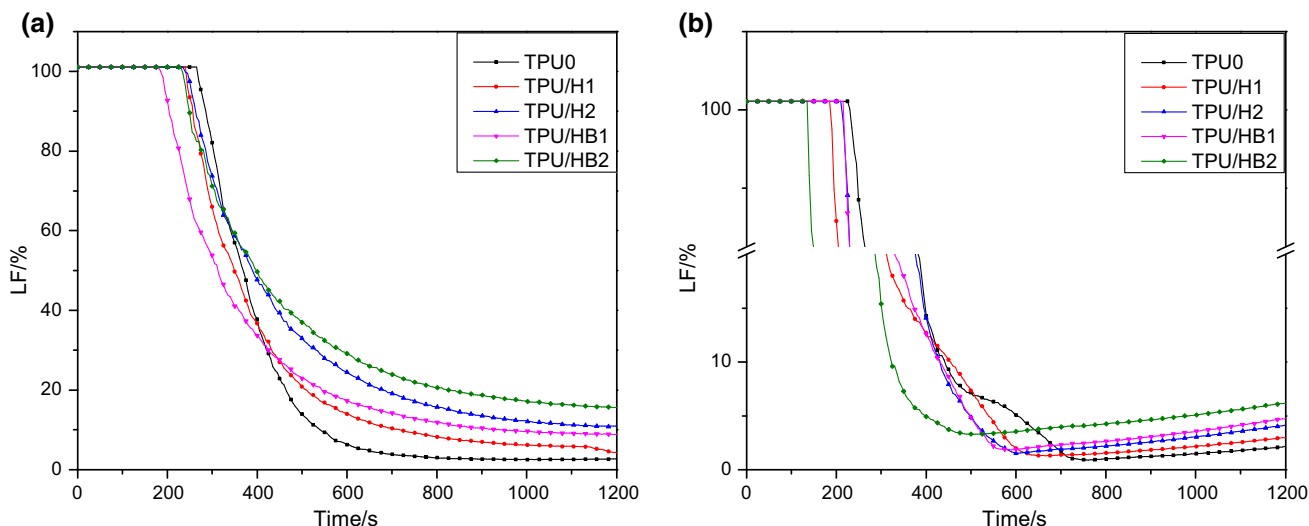


Fig. 3 LF curves of TPU composites without (a) and with flame (b)

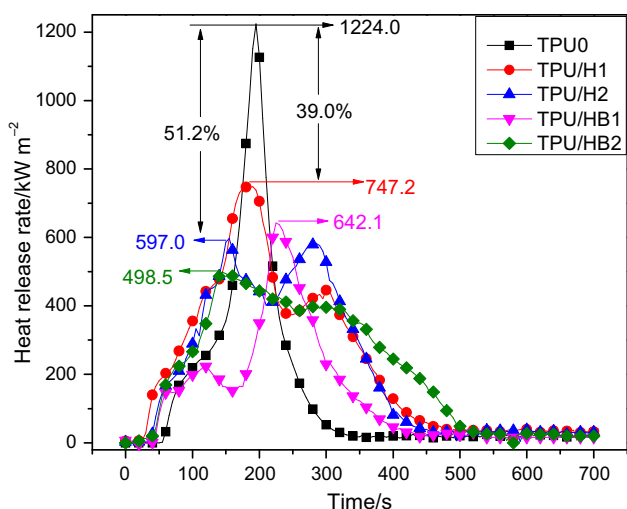


Fig. 4 Heat release rate curves of all TPU composites

containing HGM, proving that TPU/HGM@[EOOEMIm][BF₄] composites produce less combustible gas than TPU/HGM composites during the combustion process. And the conclusion can be obtained that HGM@[EOOEMIm][BF₄] is more effective than HGM in flame retardant TPU.

Smoke production rate (SPR)

SPR is a significant parameter to evaluate the smoke performance in flame retardant fields. The SPR curves are given in Fig. 6. The pSPR value of TPU0 was 0.075 m² s⁻¹, which was the highest one among all samples. And it is easily found that the pSPR values of samples with HGM@[EOOEMIm][BF₄] were lower than those of the samples with HGM. For example, the pSPR value was

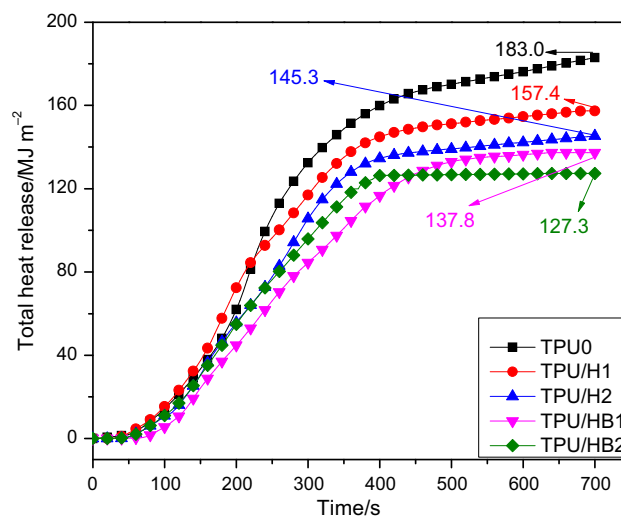


Fig. 5 Total heat release curves of all TPU composites

about 0.072 m² s⁻¹ when 0.25 mass% of HGM was added (TPU/H2); and a low pSPR value of 0.052 m² s⁻¹ was obtained when 0.25 mass% of HGM@[EOOEMIm][BF₄] was added (TPU/HB2). The pSPR value of TPU/HB2 decreased by 27.8% compared with TPU/H2, indicating the smoke suppression effect of HGM@[EOOEMIm][BF₄] is more obvious than that of HGM.

Total smoke release (TSR)

TSR curves of pure TPU and TPU composites are given in Fig. 7. Obviously, the distinction between pure TPU and the flame retardant samples was apparent after 350 s. The TSR value of pure TPU was 2009.6 m² m⁻² at the end of the test, while the TSR values of TPU/H1, TPU/H2, TPU/HB1 and

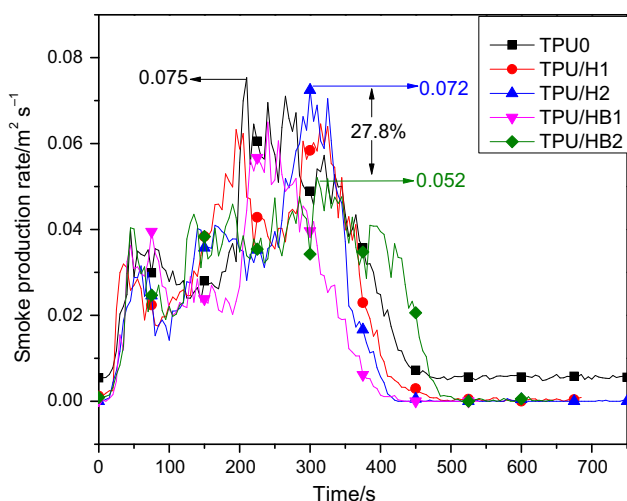


Fig. 6 Smoke production rate curves of all TPU composites

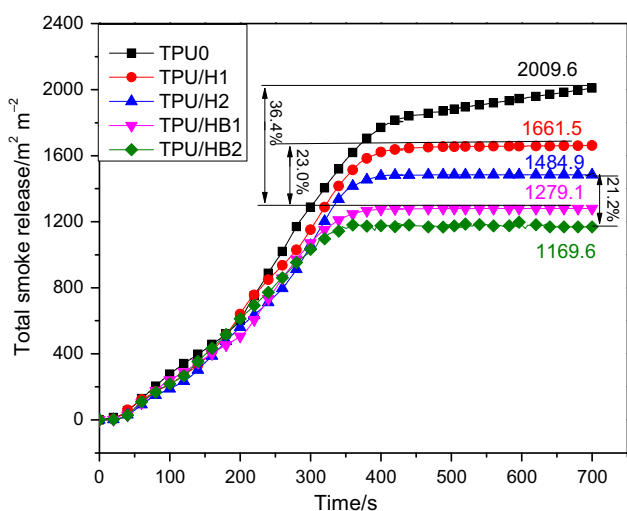


Fig. 7 Total smoke release curves of all TPU composites

TPU/HB2 were 1661.5, 1484.9, 1279.1 and 1169.6 $m^2 m^{-2}$, respectively. Remarkably, HGM@[EOOEMIm][BF₄] has better smoke suppression effect than HGM. The reason may be that HGM@[EOOEMIm][BF₄] contains [EOOEMIm][BF₄], which can catalyze the cross-linking reaction among smoke precursors to form char residue layer during the pyrolysis and combustion process. And, the products from depolymerization of TPU will be polymerized and cross-linked, and fixed in the condensed phase. Meanwhile, the carbon residue can restrain the release of smoke precursors, leading to the low TSR and SPR.

Smoke factor (SF)

The SF is calculated from the values of pHRR and TSR, which can be used to evaluate the flame retardant level of polymer materials. Figure 8 described the SF curves of all

samples. It could be seen from Fig. 8 that the SF values of flame retardant composites were much lower than that of pure TPU (2163.0 $MW m^{-2}$) at the end of the combustion. And, the SF values of the samples with 0.125 and 0.25 mass% of HGM were 1255.1 and 886.4 $MW m^{-2}$, respectively. However, when the TPU contained 0.125, 0.25 mass% HGM@[EOOEMIm][BF₄], the SF values were 1075.5 and 435.8 $MW m^{-2}$, reduced by 14.3, 50.8% compared with TPU composites containing the same loading of HGM. This demonstrates that HGM@[EOOEMIm][BF₄] can further improve the flame retardancy of TPU composites, including heat and smoke.

Mass

Figure 9 presented the mass loss curves of TPU composites. It could be seen from Fig. 9 that the residual mass of TPU composites was higher than that of pure TPU. The mass of pure TPU decreased rapidly and reached 1.2% at the end of experiment. While the residual mass of TPU/H1 and TPU/H2 was 3.8 and 4.1%, the residual mass of TPU/HB1 and TPU/HB2 was 10.6 and 14.0%, respectively. The residual mass of TPU/HB2 increased by 10% compared with that of TPU/H2 at the same loading. The main reason is that [EOOEMIm][BF₄] on the surface of HGM@[EOOEMIm][BF₄] has catalytic effect on Friedel-Crafts reaction, promoting char residue formation and creating a good physical protective barrier to prevent heat and mass transferring.

Photographs of char residue

The digital photographs for the char residues after CCT are shown in Fig. 10. It could be seen that the char residue layer of pure TPU (TPU0) was quite loose, fragile and even

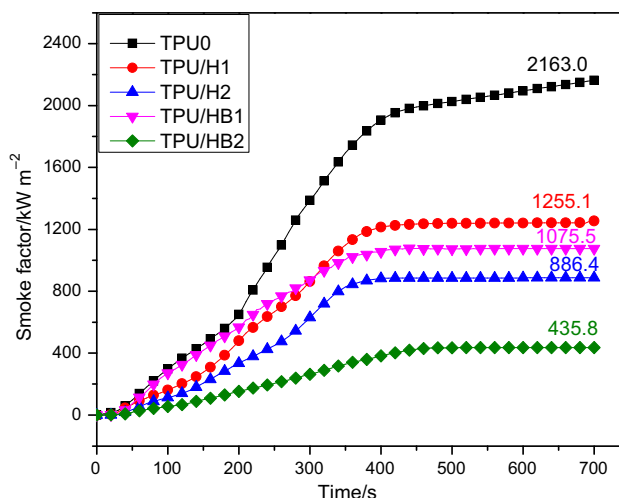


Fig. 8 Smoke factor curves of all TPU composites

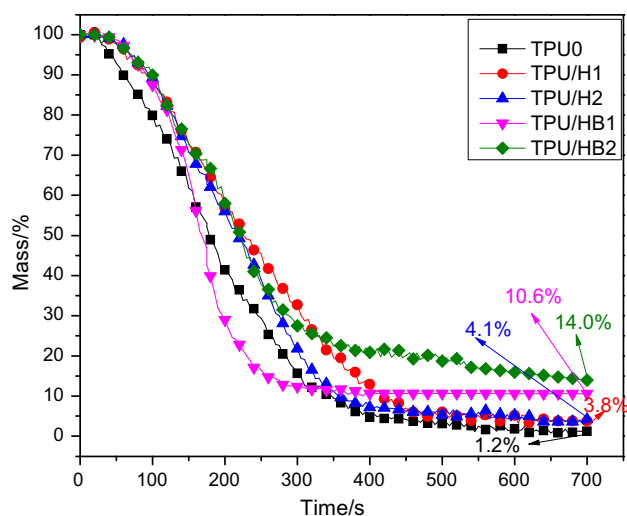


Fig. 9 Mass curves of all TPU composites

broken, which responds to the highest HRR and largest mass loss among all samples. For the samples containing HGM, the char residue layers were integrated. However, there were still some holes on the surface of the char residue layer, which could not effectively bond combustible gas and smoke particulates releasing from the underlying materials, resulting high HRR and SPR [25]. But, for the samples with HGM@[EOOEMIm][BF₄], the surface of the char layers got tight and dense with the loading of HGM@[EOOEMIm][BF₄]. Compared with the char residue from the samples with HGM, the char residue

from the samples with HGM@[EOOEMIm][BF₄] was more compact with high expansion degree. Furthermore, there is a black layer formed on the surface of the samples with HGM@[EOOEMIm][BF₄], indicating [EOOEMIm][BF₄] had played an important role in the char formation process.

The SEM-EDS was also used to investigate the microstructure of the char residues to obtain more information. And the SEM-EDS results of TPU0, TPU/H2 and TPU/HB2 are shown in Fig. 11. It can be seen there were many holes in the surface of the char residue from TPU0. And, the char residue of TPU/H2 showed a more compact appearance and smooth surface. There were almost no holes on the surface of the char residue from TPU/H2. However, the char residue from TPU/HB2 expressed the best density, thickness and mechanical strength among three samples. This can confirm that HGM@[EOOEMIm][BF₄] can promote charring and change the structure of carbon layer, forming compact carbon layer.

It could be clearly seen that the Si, B and F atoms contents on outer surface were much higher than those of inner surface from EDS result. These phenomena illustrate that HGM@[EOOEMIm][BF₄] will migrate onto the surface of the sample and catalyze TPU carbonization to form a compact char residue layer, protecting the inner matrix and reducing the amount of combustible gas and smoke-forming materials into the gas phase during combustion, leading to low HRR, THR, SPR, TSR, SF and so on. It also confirmed the results from SDT.

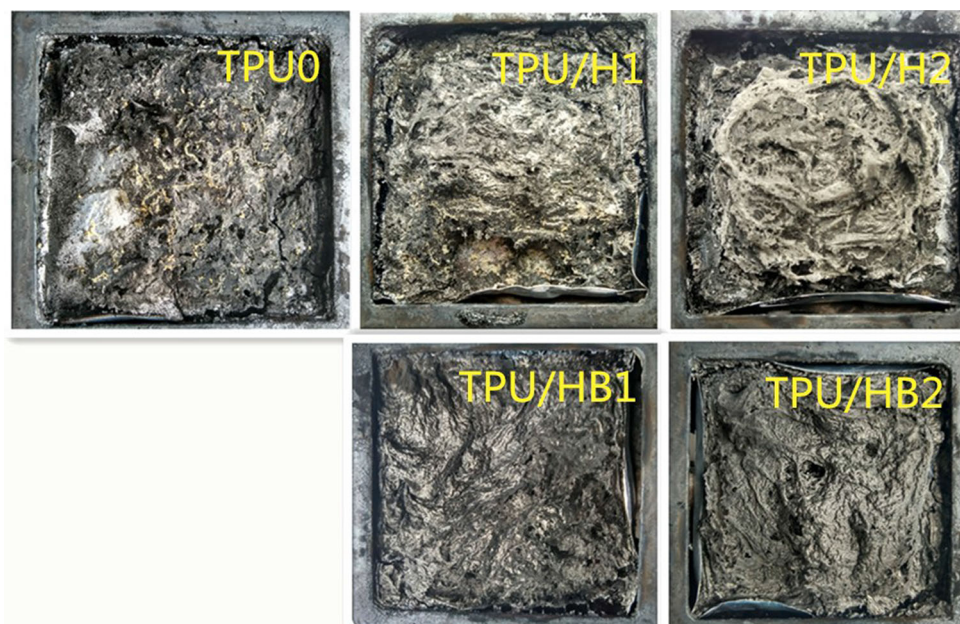


Fig. 10 Photographs of flame retardant TPU composites after CCT

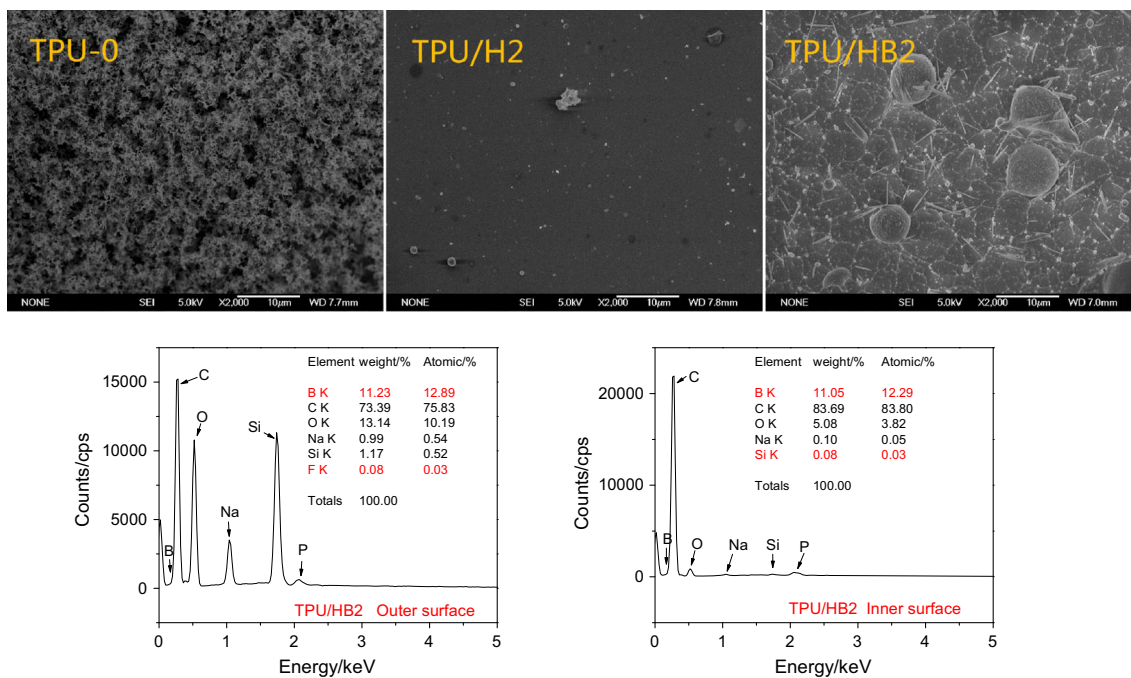


Fig. 11 The SEM-EDS results of flame retardant TPU composites after CCT

LOI and UL-94

The LOI values and UL-94 test results are presented in Fig. 12. It can be seen that pure TPU was a flammable polymeric material, and its LOI value was only 21.0%. But, the LOI values of the composites increase slightly with the increase of HGM and HGM@[EOOEMIm][BF₄]. And, the LOI values of the samples with 0.125 and 0.25 mass% of HGM were 22.5 and 23.5, respectively. However, when the TPU contained 0.125, 0.25 mass% HGM@[EOOEMIm][BF₄], the SF values were 23.0 and 25.0. The LOI values of composites containing HGM@[EOOEMIm][BF₄] were obviously higher than the composites containing the same loading of HGM. This can be explained that HGM@[EOOEMIm][BF₄] is able to improve the structure of char residue from TPU

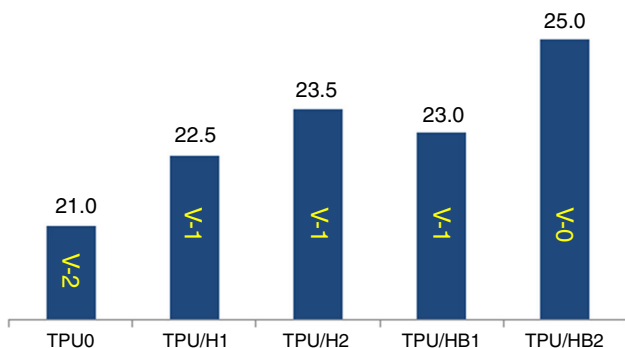


Fig. 12 The LOI and UL-94 results of TPU composites

composites, forming char residue as a protective layer on the polymer surface during degradation than HGM. Seen from the UL-94 tests, the samples with HGM or HGM@[EOOEMIm][BF₄] could reach V-1 level except pure TPU (V-2), and for the sample of TPU/HB2, the flame retardant level reached V-0, further confirming the conclusions obtained from the above experiments.

Thermogravimetric analysis (TG)

TG is a technique for rapid evaluating of the thermal stability of materials and revealing the degradation behavior of polymers at various temperatures [26–28]. The TG and DTG curves of TPU0, TPU/H2 and TPU/HB2 are shown in Fig. 13. As can be seen from TG curves in Fig. 13, the initial decomposition temperature of pure TPU was about 300 °C. And the initial decomposition temperatures of TPU/H2 and TPU/HB2 were 260 and 250 °C, which were much lower than that of pure TPU. This implies that HGM and HGM@[EOOEMIm][BF₄] can catalyze the thermal degradation of TPU and [EOOEMIm][BF₄] on the surface of HGM@[EOOEMIm][BF₄] can further increase the thermal degradation process of TPU. Combining the results of MCC test and HRR from CCT, it can be concluded there is some flammable gases formed at the initial decomposition of TPU. At the same time, char residue is formed during the pyrolysis process. The remaining mass of pure TPU was about 4.8%, while the remaining mass of TPU/H2 and TPU/HB2 was 5.6 and 9.0%, respectively. The results confirm that HGM and HGM@[EOOEMIm][BF₄] can

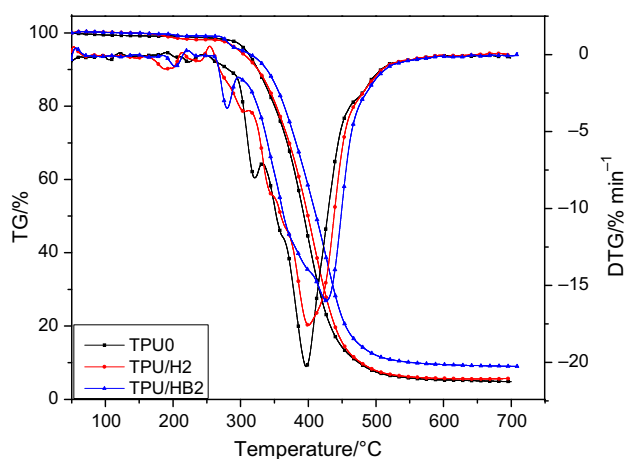


Fig. 13 TG and DTG curves of TPU composites

improve char formation during decomposition process. And, [EOOEMIm][BF₄] on the surface of HGM@[EOOEMIm][BF₄] plays an important role in the carbonization process. Seen from DTG curves in Fig. 13, the thermal degradation of TPU0 had two stages. The first stage was responsible for the rupture of the TPU main chains, and the second stage was attributed to the further destruction of the C–C and C–O bonds on the main chain [29]. For TPU/H2 and TPU/HB2, the thermal degradation of the samples also had two steps; however, the initial mass loss temperature for the TPU/H2 and TPU/HB2 was significantly lower than that for TPU0 in the first stage, which meant that the addition of HGM and HGM@[EOOEMIm][BF₄] could promote the degradation of TPU. Comparing TPU/H2 with TPU/HB2, the sample with HGM@[EOOEMIm][BF₄] was more obvious. It can be explained by the fact that [EOOEMIm][BF₄] would promote decomposition of TPU and formation of protective carbon layer which can act as barrier on the surface of the sample, resulting in low mass loss compared with TPU0 and TPU/H1 [30].

TG–IR characterization of volatile products

The volatilized products of TPU0, TPU/H2 and TPU/HB2 evolved from TG furnace during thermal decomposition process were characterized by TG–IR technique [31] and are shown in Fig. 14a–c. Seen from the infrared spectra of TPU0 in Fig. 14a, there was a strong absorption peak located at 2300–2400 cm⁻¹, which was attributed to CO₂ at about 200 °C [32, 33]. With increasing temperature, the absorption peak of CO₂ increased gradually, reaching the maximum at about 520 °C, and then began to decline gradually. In the case of TPU/H2, the absorption intensity of CO₂ reached the maximum at about 500 °C, and then declined gradually (Fig. 14b). However, for TPU/HB2, it

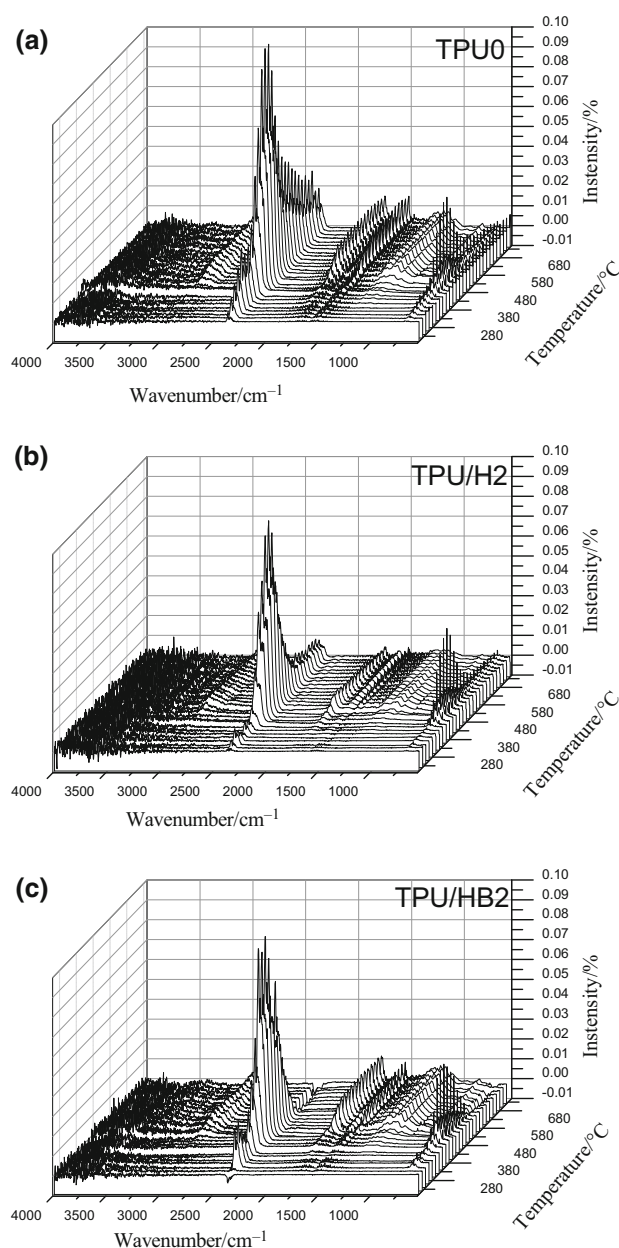


Fig. 14 FTIR spectra of volatilized products during thermal degradation of TPU composites

can be seen that the characteristic absorption of CO₂ was much lower than that from TPU/H2 during the whole thermal decomposition process (Fig. 14c). The peak of CO₂ disappeared at about 600 °C, which confirmed that the decomposition of char residue from the sample with HGM@[EOOEMIm][BF₄] carried out completely. It is more interesting that the main absorption peak of H₂O (3700 cm⁻¹) from TPU/H1 and TPU/HB2 appeared at lower temperature than that from pure TPU. And, [EOOEMIm][BF₄] on the surface of HGM@[EOOEMIm][BF₄] can further promote the production of H₂O compared

with HGM, which is good for improving the flame retardancy of the composites [34, 35].

Conclusions

HGM@[EOOEMIm][BF₄], as a new type of flame retardant, was prepared and used in TPU in this paper. And, the flame retardant properties and thermal degradation behaviors of TPU were investigated by various techniques. It has been found that HGM@[EOOEMIm][BF₄] can change the thermal degradation process of TPU, catalyze TPU decomposed to some flammable gases, CO₂, H₂O, and some other compounds including char residue. The flammable gases lead the ignition time and temperature of the sample to be short. It can be confirmed that HGM@[EOOEMIm][BF₄] can migrate onto the surface of the sample, promoting a compact char residue layer formation; furthermore, both HGM and [EOOEMIm][BF₄] can catalyze carbonization of TPU to form char residue layer. The char formation has played a key role for the flame retardant improvement in TPU in the combustion process. Based on the barrier effect from char residue layer, the production of flammable gases and smoke particles was reduced, leading to low HRR, THR, SPR, TSR, SF, mass loss and high LF. The above results indicated that HGM@[EOOEMIm][PF₆] could provide some polymer with high fire safety and might have a wide application prospect in flame retardant fields.

Acknowledgements The authors gratefully acknowledge the National Natural Science Foundation of China (No. 51776101, No.51206084), the Major Special Projects of Science and Technology from Shandong Province (2015ZDZX11011), the Natural Science Foundation of Shandong Province (ZR2017MB016), and the Project of the State Administration of Work Safety (shandong-0039-2017AQ).

References

1. Tabuani D, Belluccia F, Camino G. Flame retarded thermoplastic polyurethane (TPU) for cable jacketing application. *Polym Degrad Stab.* 2012;97:2594–601.
2. Chen X, Ma C, Jiao C. Enhancement of flame-retardant performance of thermoplastic polyurethane with the incorporation of aluminum hypophosphite and iron-graphene. *Polym Degrad Stab.* 2016;129:275–85.
3. Pinto U, Visconte L, Gallo J, Nunes R. Flame retardancy in thermoplastic polyurethane elastomers (TPU) with mica and aluminum trihydrate (ATH). *Polym Degrad Stab.* 2000;69:257–60.
4. Li H, Ning N, Zhang L, Wang Y, Liang W, Tian M. Different flame retardancy effects and mechanisms of aluminium phosphinate in PPO, TPU and PP. *Polym Degrad Stab.* 2014;105:86–95.
5. Chen X, Jiang Y, Jiao C. Smoke suppression properties of ferrite yellow on flame retardant thermoplastic polyurethane based on ammonium polyphosphate. *J Therm Anal Calorim.* 2015;120:1493–501.
6. Jiao C, Zhao X, Song W, Chen X. Synergistic flame retardant and smoke suppression effects of ferrous powder with ammonium polyphosphate in thermoplastic polyurethane composites. *J Therm Anal Calorim.* 2015;120:1173–81.
7. Liu L, Hu J, Zhuo J, Jiao C, Chen X, Li S. Synergistic flame retardant effects between hollow glass microspheres and magnesium hydroxide in ethylene-vinyl acetate composites. *Polym Degrad Stab.* 2014;104:87–94.
8. Geleil A, Hall M, Shelby J. Hollow glass microspheres for use in radiation shielding. *J Non-Cryst Solids.* 2006;352:620–5.
9. Hu Y, Mei R, An Z, Zhang J. Silicon rubber/hollow glass microsphere composites: influence of broken hollow glass microsphere on mechanical and thermal insulation property. *Compos Sci Technol.* 2013;79:64–9.
10. Brow R, Schmitt M. A survey of energy and environmental applications of glass. *J Eur Ceram Soc.* 2009;29:1193–201.
11. Verweij H, With G, Veeneman D. Hollow glass microsphere composites: preparation and properties. *J Mater Sci.* 1985;20:1069–78.
12. Li B, Yuan J, An Z, Zhang J. Effect of microstructure and physical parameters of hollow glass microsphere on insulation performance. *Mater Lett.* 2011;65:1992–4.
13. Liang J. Tensile and impact properties of hollow glass bead-filled PVC composites. *Macromol Mater Eng.* 2002;287:588–91.
14. Kim H, Khamis M. Fracture and impact behaviours of hollow microsphere/epoxy resin composites. *Compos A.* 2000;32:1311–7.
15. Chen X, Jiang Y, Jiao C. Synergistic effects between hollow glass microsphere and ammonium polyphosphate on flame-retardant thermoplastic polyurethane. *J Therm Anal Calorim.* 2014;117:857–66.
16. Jiao C, Wang H, Li S, Chen X. Fire hazard reduction of hollow glass microspheres in thermoplastic polyurethane composites. *J Hazard Mater.* 2017;332:176–84.
17. Yang X, Ge N, Hu L, Gui H, Wang Z, Ding Y. Synthesis of a novel ionic liquid containing phosphorus and its application in intumescent flame retardant polypropylene system. *Polym Adv Technol.* 2013;24:568–75.
18. Chen S, Li J, Zhu Y, Guo Z, Su S. Increasing the efficiency of intumescent flame retardant polypropylene catalyzed by polyoxometalate based ionic liquid. *J Mater Chem A.* 2013;1:15242–6.
19. He Y, Zhang Q, Zhan X, Cheng D, Chen F. Synthesis of efficient SBA-15 immobilized ionic liquid catalyst and its performance for Friedel–Crafts reaction. *Catal Today.* 2016;276:112–20.
20. Ran S, Guo Z, Han L, Fang Z. Effect of Friedel–Crafts reaction on the thermal stability and flammability of high-density polyethylene/brominated polystyrene/graphene nanoplatelet composites. *Polym Int.* 2014;63:1835–41.
21. Ge H, Tang G, Hu W, Wang B, Pan Y, Song L, Hu Y. Aluminum hypophosphite microencapsulated to improve its safety and application to flame retardant polyamide 6. *J Hazard Mater.* 2015;294:186–94.
22. Chen X, Li M, Zhuo J, Ma C, Jiao C. Influence of Fe₂O₃ on smoke suppression and thermal degradation properties in intumescent flame-retardant silicone rubber. *J Therm Anal Calorim.* 2015;123:439–48.
23. Fang S, Hu Y, Song L. Mechanical properties, fire performance and thermal stability of magnesium hydroxide sulfate hydrate whiskers flame retardant silicone rubber. *J Mater Sci.* 2008;43:1057–62.
24. Jiao C, Zhao L, Chen X. Preparation of modified hollow glass microspheres using Fe₂O₃ and its flame retardant properties in thermoplastic polyurethane. *J Therm Anal Calorim.* 2017;12:2101–12.
25. Pan H, Wang W, Pan Y, Song L, Hu Y, Liew K. Formation of layer-by-layer assembled titanate nanotubes filled coating on flexible polyurethane foam with improved flame retardant and

- smoke suppression properties. *ACS Appl Mater Interfaces*. 2015;7:101–11.
26. Zhou K, Tang G, Jiang S, Gui Z, Hu Y. Combination effect of MoS₂ with aluminum hypophosphite in flame retardant ethylene-vinyl acetate composites. *RSC Adv*. 2016;6:37672–80.
 27. Aslzadeh M, Abdouss M. Preparation and characterization of new flame retardant polyurethane composite and nanocomposite. *J Appl Polym Sci*. 2013;127:1683–90.
 28. Tang C, Yan H, Li S. Effects of novel polyhedral oligomeric silsesquioxane containing hydroxyl group and epoxy group on the dicyclopentadiene bisphenol dicyanate ester composites. *Polym Test*. 2007;59:316–27.
 29. Chen X, Jiang Y, Liu J, Jiao C, Qian Y, Li S. Smoke suppression properties of fumed silica on flame-retardant thermoplastic polyurethane based on ammonium polyphosphate. *J Therm Anal Calorim*. 2015;120:1493–501.
 30. Fang G, Li H, Chen Z, Liu X. Preparation and characterization of flame retardant n-hexadecane/silicon dioxide composites as thermal energy storage materials. *J Hazard Mater*. 2010;181:1004–9.
 31. Liu Q, Wang S, Zheng Y, Luo Z, Cen K. Mechanism study of wood lignin pyrolysis by using TG–FTIR analysis. *J Anal Appl Pyrolysis*. 2008;82:170–7.
 32. Chen X, Ma C, Jiao C. Synergistic effects between iron-graphene and ammonium polyphosphate in flame-retardant thermoplastic polyurethane. *J Therm Anal Calorim*. 2016;126:633–42.
 33. Li B, Lv W, Zhang Q, Wang T, Ma L. Pyrolysis and catalytic pyrolysis of industrial lignins by TG–FTIR: kinetics and products. *J Anal Appl Pyrolysis*. 2014;108:295–300.
 34. Chen X, Huo L, Jiao C, Li S. TG–FTIR characterization of volatile compounds from flame retardant polyurethane foams materials. *J Anal Appl Pyrolysis*. 2013;100:186–91.
 35. Xu T, Huang X. A TG–FTIR investigation into smoke suppression mechanism of magnesium hydroxide in asphalt combustion process. *J Anal Appl Pyrolysis*. 2010;87:217–23.